A Technique for Subpixel Analysis of Dynamic Mangrove Ecosystems With Time-Series Hyperspectral Image Data

Somdatta Chakravortty, Jun Li, *Senior Member, IEEE*, and Antonio Plaza, *Fellow, IEEE*

***Abstract*—Changes in mangrove forests are mostly caused by natural disasters, anthropogenic forces, and uncontrolled population growth. These phenomena often lead to a strong competition between existing mangrove species for their survival. Due to its enhanced spectral resolution, remotely sensed hyperspectral image data can play an important role in the task of mapping and monitoring changes in mangrove forests. In this paper, we use EO-1 Hyperion hyperspectral data to model the abundance of pure and mixed mangrove species at subpixel levels. This information is then used to analyze the interspecies competition in a study area over a period of time. Different characteristics, including the rate of growth, rate of reproduction, mortality rate, and other processes that control the coexistence of plant species are discussed. The obtained results, verified through field visits, illustrate that the proposed approach can interpret the dominance of certain mangrove species and provide insights about their state of equilibrium or disequilibrium over a fixed time frame.**

***Index Terms*—Change detection, competition models, hyperspectral data, mangrove systems.**

I. Introduction

THE Sunderban mangrove forest is a threatened ecosystem and an ecological hotspot of India. The biophysical buffer mechanism of the coastal Sunderban itself has experienced significant spatial and temporal changes, owing to different factors. These disturbances (natural and/or anthropogenic) cause ecological degradation that tends to alter the dynamic state of the ecosystem. Hence, continuous up-to-date monitoring needs to be undertaken, using effective mechanisms able to find out the nature and distribution pattern of mangrove species, in order to establish a holistic management plan for the sustainability of this ecosystem.

Manuscript received June 7, 2017; revised November 15, 2017; accepted December 1, 2017. Date of publication December 28, 2017; date of current version April 11, 2018. This work was supported by the National Natural Science Foundation of China under Grant 61771496. *(Corresponding author: Jun Li.)*

S. Chakravortty is with the Department of Information Technology, Government College of Engineering and Ceramic Technology, Kolkata 700010, India (e-mail: csomdatta@rediffmail.com).

J. Li is with the Guangdong Provincial Key Laboratory for Urbanization and Geo-simulation, School of Geography and Planning, Sun Yat- Sen University, Guangzhou 510275, China (e-mail: lijun48@mail.sysu.edu.cn).

A. Plaza is with the Department of Technology of Computers and Communications, University of Extremadura, Badajoz 06071, Spain (e-mail: aplaza@unex.es).

Color versions of one or more of the figures in this paper are available online at http://ieeexplore.ieee.org.

Digital Object Identifier 10.1109/JSTARS.2017.2782324

The continuous onslaught of natural and/or anthropogenic perturbations on river-sea interface zones motivates adaptive responses within mangrove species, e.g., through their rapid regeneration for survival. In this process, different mangrove communities tend to interact with each other. These interactions are competitive as well as mutual. This work intends to analyze such interactions using information extraction techniques applied to remotely sensed hyperspectral images [1]–[3]. There has been extensive work in the study of mangroves with hyperspectral data. In [4], the authors used Hyperion data to classify five different species of mangroves. In [28], the authors identified mangrove species using linear and non-linear spectral unmixing of hyperspectral data. Wang *et al*. [5] performed textural-based classification of mangrove species with Hyperion data. Viennois *et al*. [6] performed multitemporal analysis of high-spatial-resolution data for identification of mangrove species.

Dynamic mangrove ecosystems have been modeled through physical monitoring of dense forests. Ground-truth studies [7], [8] have used density-dependent mortality and light-dependent colonization to analyze the coexistence of species and derived competition models based on the competitive ability and mortality of mangrove species [8]. Other studies monitored changes in vegetation by analyzing other kinds of satellite image data in different time periods. Vegetation indices, such as NDVI, have been calculated to measure the greenness of a particular area [9]. For instance, Tilman evaluated the competition between two species by analyzing parameters such as colonization and dispersal rate [10]. Changes have been detected using techniques such as image differencing by subtracting intensity values in pairs of images collected at two different time periods [11]. The calculation of the band ratio of pixels has been used in other studies to identify changes [12]. Change vector analysis has been also used to calculate the magnitude of spectral changes among different images [13]. Other studies have applied principal component analysis (PCA), independent component analysis (ICA), and the k-means algorithm for unsupervised change detection using hyperspectral data [14]–[17]. Linear techniques have also been used to predict a space-invariant affine transformation between image pairs [18], [19]. There have also been studies focused on automatic change detection in high-resolution remote sensing images, by using multiple classifier systems and spectral-spatial features [20]. Sparse unmixing-based change detection studies have also been conducted on multi-temporal hyperspectral images [21].

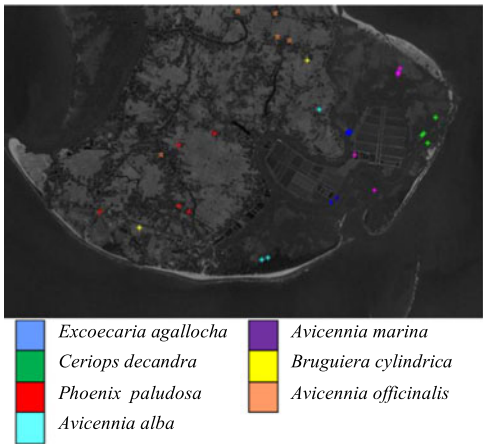

Fig. 1. High resolution cartosat-1 Image of the study area with sampling locations of pure patches.

From the aforementioned literature survey, it can be deducted that the dynamics of mangrove ecosystems have only been studied through physical monitoring and ground surveys. Predicting the outcome of competitive interactions between mangrove species from satellite data in general (and from hyperspectral imagery in particular) can greatly overcome the limitations of ground surveys. In this regard, an original contribution of this work is to exploit image derived fractional abundance values (obtained from spectral unmixing of hyperspectral data) in the characterization of dynamic mangrove ecosystems. Our work also uniquely exploits a popular ecological model, namely the Lotka–Volterra competition model, to explain the inherent intra- and interspecies competitions that happen in natural forests over a time period [22]–[24]. This is accomplished by a detailed analysis of image-derived fractional abundances obtained from linear spectral unmixing, which has helped us to determine the dominance of certain mangrove species. The stability and dynamics of mangrove species within different mixed patches have also been analyzed to predict species coexistence, dominance and/or mutual exclusion over a period of time.

II. Study Area

As a case study, the mangrove habitats of Henry Island, located in the Sunderban Biosphere Reserve of West Bengal have been selected for evaluation purposes, where Fig. 1 shows a high resolution image acquired by the Cartosat-1 sensor over the study area, along with the sampling locations of pure mangrove species. The choice of this study area has been performed after considering the fact that Sunderban harbors are an example of a rich and bio-diverse mangrove community, with a wide array of ecologically rare, endangered, and endemic mangrove species. Specifically, Henry Island is dominated by species such as *Avicennia*, *Ceriops*, and *Rhizophora*. There are also mixed mangrove forest species of *Bruguiera cylindrica, Aegialitis*, and *Excoecaria agallocha.*

A. Data Acquisition

An EO-1 Hyperion (hyperspectral) image of the study area has been obtained from the USGS Earth Resources Observation and Science (EROS) Center by placing a data acquisition request to the satellite data provider. The Hyperion sensor acquired the data on May 27, 2011, and November 23, 2014, and was downloaded from their database.

B. Data Preprocessing

For the Hyperion hyperspectral data, first, we performed atmospheric and geometric correction before the analysis of the interspecies competition.

1) Atmospheric Correction: The Fast Line-of-Sight Atmospheric Analysis of Spectral Hypercubes (FLAASH) model available in ENVI software has been used for atmospheric correction, to convert the radiance values in the image to reflectance values. FLAASH is an atmospheric correction tool that corrects wavelengths in the visible through near-infrared and shortwave infrared regions, up to 3 μm. Unlike many other atmospheric correction programs that interpolate radiation transfer properties from a pre-calculated database of modeling results, FLAASH incorporates the MODTRAN4 radiation transfer code. Water vapor and aerosol retrieval are only possible when the image contains bands in appropriate wavelength positions. In addition, FLAASH can correct images collected in either vertical (nadir) or slant-viewing (off-nadir) geometries.

2) Geometric Correction: Geometric correction helps to locate the accurate position of each pixel in a geographical or map coordinate. The image-to-image registration method has been selected in this paper after considering the characteristics of available reference data and distortion in our image data. This is a translation and rotation alignment process by means of which two images of similar geometry, and of the same geographic area, are positioned coincident with respect to one another so that the corresponding pixels in the same ground area appear in the same place on the registered images [25]. A georeferenced Hyperion image of the study area, acquired by USGS, has been used as a reference image, which will be used to match the un-rectified image. The projection for the study area is UTM at Zone 45 (North) and Datum: WGS-84.

C. Ground Survey

A ground survey of the study area has been conducted to identify and collect samples of mangrove species. The field visit for initial ground-truth data collection was performed in the month of June 2011, immediately after the acquisition of the image data. GPS data (with accuracy of 4 m) have also been used to precisely locate the geographical coordinates of the study trail. In the initial visit for ground-truth data collection, several quadrats of 30 m $\times$ 30 m (equal to the spatial resolution of the Hyperion imagery) were defined to estimate the presence of dominant mangrove species on the ground. Quadrat survey is a method for analysis of biodiversity. A series of quadrats of fixed size have been positioned in our study area, and species within the quadrats have been recognized and noted. The abundances of species detected at the study area are estimated by means of the number of samples per quadrat and the size of the quadrat area. Thirty samples of pure and twenty samples of mixed covers of mangrove species were collected and plotted on the geometrically corrected hyperspectral imagery with the help of GPS data [25]. It should be noted that due to the mixing nature of mangrove species, it is very difficult to have pure

TABLE I
GROUND CONTROL POINTS OF THE PATCHES OF PURE MANGROVE SPECIES COLLECTED DURING THE GROUND SURVEY

Name of Mangrove Species Identified	Latitude (N)	Longitude (E)
Excoecaria agallocha	21°34′9.40"	88°17′10.68"
	21°34'42.52"	88°17'17.23"
	21°34'42.51"	88°17'18.27"
	21°34'41.55"	88°17'16.18"
	21°34'41.55"	88°17'17.22"
	21°34′7.47"	88°17′7.53"
Ceriops decandra	21°34′48.99"	88°18′3.18"
	21°34'41.24"	88°17'56.85"
	21°34'40.27"	88°17'55.80"
	21°34'36.34"	88°17'58.90"
Phoenix paludosa	21°34′3.17"	88°15′52.40"
	21°34'42.09"	88°16'6.30"
	21°34'36.38"	88°15'47.47"
	21°34'6.14"	88°15'47.21"
	21°34'3.53"	88°15'5.47"
Avicennia alba	21°33′39.46"	88°16′30.78"
	21°34'53.37"	88°17'1.68"
	21°33'40.42"	88°16'33.92"
Avicennia marina	21°34′13.15"	88°17′30.53"
	21°35'13.53"	88°17'44.62"
	21°35'11.58"	88°17'43.56"
	21°35'10.61"	88°17'43.55"
	21°34'30.79"	88°17'20.25"
Bruguiera cylindrica	21°33′55.56"	88°15′26.26"
	21°35'17.81"	88°16'55.64"
Avicennia officinalis	21°34′31.57"	88°15′38.04"
	21°35'42.48"	88°16'19.34"
	21°35'41.35"	88°16'39.15"
	21°35'29.64"	88°16'40.09"
	21°35'27.64"	88°16'46.33"

regions with one single mangrove specie. Therefore, in this paper, the pure or mixed nature of each cover was measured based on the mangrove trees crown size. Specifically, in this study, the quadrats that have the presence of more than 80% coverage of tree crown of a particular species were considered as pure stands of the mangrove species. In turn, the quadrats in which none of the mangrove species have 80% presence were considered as mixed mangrove patches. These points were used as checkpoints to assess the accuracy between the image-derived and field measured values of the mangrove species. The ground survey for validation of unmixing results was repeated in May 2012 and June 2013. As our study involves change detection and identification of dominant mangrove species in the eco-system within a time period, change in humidity and tidal variations does not significantly affect our results. Specifically, there is no report of any major change in the routine tidal variations over the three year time period. Moreover, there has not been any occurrence of cyclonic storms that may have resulted in a major land cover change. Also, it is difficult to obtain time series Hyperion data of the study area for different seasons in a year to monitor changing humidity and tidal conditions from time to time. It is known that natural changes in forest cover do not occur very frequently. A minimum five- to ten-year time span is required to note significant and visible changes in the ecosystem. Due to the unavailability of seasonal Hyperion data, we used the images acquired in two years (2011 and 2014) for our analysis and research.

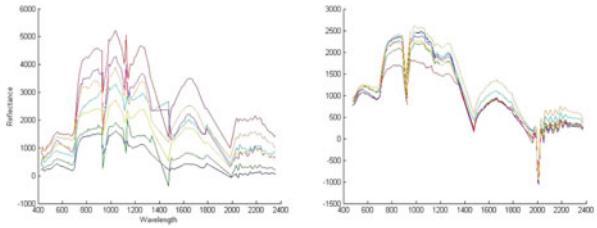

Fig. 2. Endmember signatures extracted via N-FINDR for the 2011 (left) and 2014 (right) data.

For illustrative purpose, Table I displays some of the geographic coordinates of the patches that have been considered as pure mangrove species in the study area during the ground survey.

III. METHODOLOGY

In this section, we will present the proposed technique for the analysis of Mangrove ecosystems by using the aforementioned EO-1 Hyperion data. First, we perform spectral unmixing to detect the mangrove endmembers and their fractional abundances in each pixel. Then, we exploit an ecodynamic model to characterize the data.

A. Spectral Unmixing

Spectral libraries comprising spectral signatures of mangrove species are not available in the literature till date, mainly due to the fact that supervised identification of mangrove species in mangrove forests is very risky. Most of the mangrove forests in the Sunderban region are dense and fall under the core forest zone having presence of man eating Royal Bengal Tigers, crocodiles and poisonous snakes among other wild animals. It is quite risky and difficult to collect mangrove spectra from these areas on foot. In such a situation, we apply unsupervised endmember detection algorithms on the hyperspectral data as a plausible solution to the extraction of unknown spectra of pure pixels (mangrove species) from the given hyperspectral forest scenes. To identify distinct endmembers (unique signatures of mangrove species), an unsupervised endmember detection algorithm (N-FINDR) has been applied to the hyperspectral imagery [26]. The spectral profile of endmembers extracted from the hyperspectral images of 2011 and 2014 is shown in Fig. 2, while Fig. 3 demonstrates the image derived spectra (in shiny red color) from the 2011 data and the ground spectra (in other colors) of Mangrove species. As it can be observed from Fig. 3, the extracted spectra exhibit good correlation with the ground ones.

It can also be observed from Figs. 2 and 3 that the bands between 550 and 600 nm in the green region, 700 and 900 nm in the near-infrared region, and 1650 and 1700 nm in the shortwave infrared region separate the mangrove species best. The mangrove species mostly differ in leaf color, canopy structure, and leaf water content. As leaf color is dependent on its chlorophyll content, low chlorophyll shows higher reflectance and high chlorophyll shows lower reflectance in the green bands. *E. agallocha* has more chlorophyll content than *Phoenix paludosa* and thus has lower reflectance than *Phoenix*. Mangrove species such as *Ceriops decandra* and *P. paludosa* have lower canopy

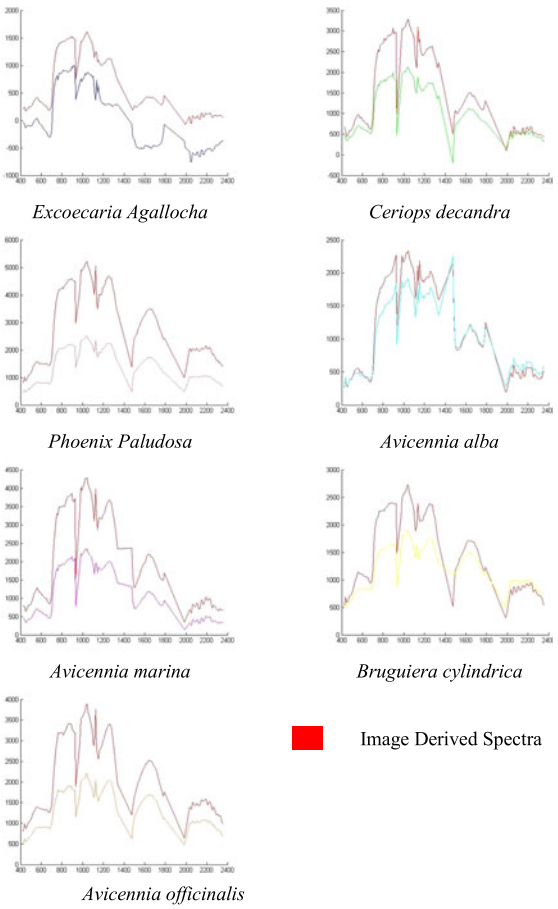

Fig. 3. The image derived spectra (in shiny red color) from the 2011 data and the ground spectra (in other colors) of mangrove species.

height as compared to tall trees such as *Avicennia marina* and *E. agallocha* that can be well differentiated in the near-infrared region. Mangrove species such as *E. agallocha* has more leaf water content as compared to *Phoenix* and hence shows more absorption in the SWIR bands than others. The endmembers extracted by N-FINDR are fed into the fully constrained linear spectral unmixing (FCLSU) algorithm to derive the fractional abundances of pixels in the hyperspectral image [29], [30]. The linear mixture model is based on the principle that if the total surface area is divided proportionally according to the fractional abundances of the constituent substances, then the reflected radiation is also proportional to the associated materials [30]–[33]. Here, we include the so-called nonnegative and sum-to-one constraints. That is, the target abundance fractions are constrained to the range of [0, 1].

Furthermore, Fig. 4 shows the fractional abundance distribution maps of the mangrove species obtained after using linear spectral mixture analysis for the data sets in 2011 and 2014. The integrated fractional abundance image displaying mangrove species in the study area with more than 50% dominance within a pixel area is also displayed in Fig. 4. This figure shows the mangrove species distribution map obtained after using linear spectral mixture analysis for the data sets in 2011 (with 50%+ abundance), 2011 (with 80% + abundance), and 2014 (with 50%+ abundance). We have assumed 80% dominance of a particular mangrove endmember within a pixel area to consider it

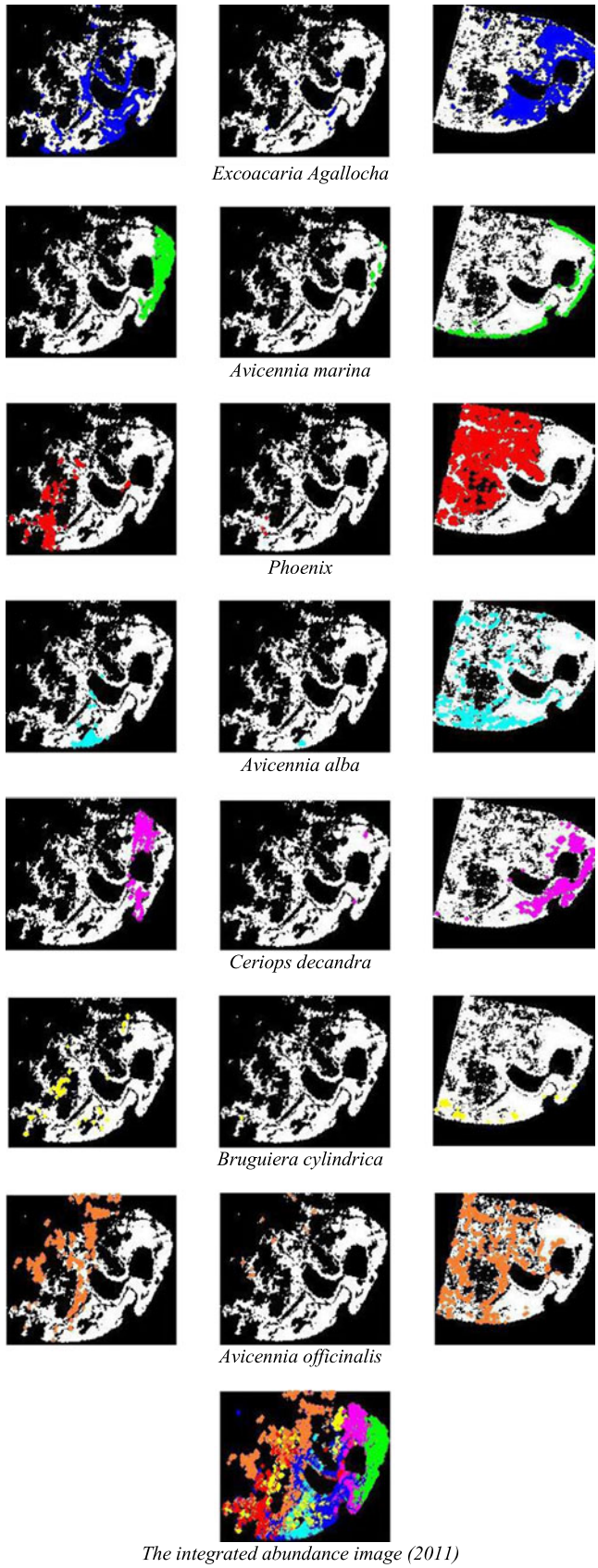

Fig. 4. Mangrove species distribution maps obtained via the linear spectral mixture analysis by using the extracted endmbmers for the data sets in 2011 with 50%+ abundance (left)), with 80% + abundance (middle) and in 2014 with 50%+ abundance (right).

a pure patch. As there are some mangrove species such as *B. cylindrica* and *Phoenix* that do not show any presence of pure patches, we have also shown 50%+ dominance side by side to indicate their presence.

It also should be noted that the 2011 hyperspectral image has clouds on the western and northern side; hence, portions of the mangrove forest under the cloud cover has been masked out. These masked out areas appear as white gaps in between the thick forest cover, which makes the mangrove species in the 2011 image appear in lesser abundance than its actual distribution. However, the 2014 image displays the correct abundance distribution of mangrove species in that year.

B. Description of Ecodynamics Model

The model assumes that mangrove species spatially adjacent to each other compete with each other to survive within the limited resources. The fractional abundances of each species (derived from FCLSU) for each pixel area (900 m^2) of Hyperion data represent its extent of occurrence within the area. It is essential to calculate the survival capacity of a certain species over the pixel area to predict its dominance over other species. However, the values vary with time. On the one hand, they depend upon the type of species, competition, and the physical environment around them. On the other hand, the survival capacity of mangrove species is also dependent upon its rate of reproduction, rate of mortality, and rate of growth over a period of time. The survival capacity k_i of species *i* is calculated as

$$k_i = \frac{(a_i - \mu_i) * p_i}{a_i} \tag{1}$$

where a_i is the rate of reproduction, μ_i is the rate of mortality, and p_i is the fractional abundance of species *i* in a pixel area over the considered years (2011 or 2014). Let $r_i = a_i - \mu_i$ be the growth rate, then we have

$$a_i = \mu_i + r_i \tag{2}$$

and

$$k_i = \frac{r_i * p_i}{a_i} \tag{3}$$

where r_i and μ_i can be calculated on the basis of the increase and decrease in species population size (i.e., the difference in fractional abundance occupied by species *i*) with time, respectively. Following the work in [33], the growth of species over a period of time is assumed to have minimum mortality rate (0.0005) and the mortality is also assumed to have minimum growth rate (0.0005). The *importance value* (*IV*) of a particular species within the pixel area is an index that defines the relative dominance of a species *i* in the mangrove community among other species. In this paper, it is expressed as

$$\mathrm{IV}_i = \frac{A_i}{\sum_{i=1}^{m} A} * 100 \tag{4}$$

where A_i is the fractional abundance area occupied by species *i* and *m* is the total number of species present within the pixel area.

Another important parameter to predict the species response in competition with other species is the *competition factor* (CF), defined as spatial and time-based probability of occurrence of species *i* imposed by species *j* and vice versa. As interspecies competition has been considered in this study, pair-wise interaction between species *i* with *j* and vice versa have been considered. Let β_{ij} be the CF of species *i* by species *j*, which can be expressed as the IV of each species divided by 100 [34], as follows:

$$\beta_{ij} = \frac{\mathrm{IV}_{ij}}{3 * 100} \tag{5}$$

where IV_{ij} is the IV of species *i* with respect to species *j*. Depending on the CF and the survival capacity of the species, the competition coefficient is then calculated based on the reproduction rate of the species in order to capture the interaction between various species. If we denote the competition coefficient between two species (*i* and *j*) by a_{ij}, the reproduction rate of a species by f_i, and the survival capacity by k_i, then a_{ij} can be expressed as

$$a_{ij=}\frac{(2 * \beta_{ij} * k_i) + f_i}{f_i}. \tag{6}$$

The competition coefficient of species *i* with respect to species *j*, a_{ij} is thus dependent upon its reproduction rate, survival capacity and CF and would vary with a_{ji} as every species has its own calculated parameters. The combination of species interacting with each other may exhibit a state of equilibrium or disequilibrium due to competition among themselves or other external influences. The inequalities used to model the stability or instability due to pair-wise interactions between mangrove species are displayed in Table II, where *k* stands for survival capacity and a_{ij}, a_{ji} are the competition coefficients.

TABLE II
INEQUALITIES USED TO INTERPRET THE STATE OF EQUILIBRIUM OF MANGROVE SPECIES

Inequalities	$k_i > (k_j/a_{ji})$	$k_i < (k_j/a_{ji})$
$k_j > (k_i/a_{ij})$	Unstable state	Species *j* wins
$k_j < (k_i/a_{ij})$	Species *i* wins	Stable state

C. Modeling the Dynamics of Mangrove Ecosystems Using Lotka–Volterra Model

Equilibrium analysis of ecological systems is an important tool for analyzing the system behavior. The differential equations of the competitive Lotka–Volterra model are used in this paper for analyzing the equilibrium of dynamic mangrove ecosystems [33]. This model has been generalized to the number of species competing against each other and calculates the growth rate of a species in competition with the remaining species within the considered area, as follows:

$$\frac{dA_i}{dt} = r_i A_i \left(1 - \sum\nolimits_{j=1}^{n} a_{ij} A_j\right) \tag{7}$$

where $\frac{dA_i}{dt}$ is the growth rate of species *i* with respect to time *t*, A_i is the fractional abundance of a species *i* in a particular pixel location, A_j is the fractional abundances of species *j* (*j* is different for *i*) present in the same pixel area, and *n* is the total number of species present in a particular pixel location. It should be noted that in (6), the value of a_{ii} is a self-interacting

TABLE III
GROWTH RATE, MORTALITY RATE, AND REPRODUCTION RATE OF RELEVANT MANGROVE SPECIES

Geographic Location	Name of Species	Growth Rate	Mortality Rate	Reproduction Rate
A	*E. agallocha*	0.01978	0.0005*	0.02028
	A.officinalis	0.0005#	0.0090	0.0095
	A. alba	0.0030	0.0005*	0.0035
	B. cylindrica	0.0005#	0.0041	0.0046
B	*E.agallocha*	0.0157	0.0005*	0.0162
	C. decandra	0.0134	0.0005*	0.0139
	P.paludosa	0.0275	0.0005*	0.028
C	*E. agallocha*	0.0526	0.0005*	0.0531
	A. alba	0.0005#	0.0081	0.0086
	B. cylindrica	0.0005#	0.0039	0.0044
	A. officinalis	0.0531	0.0005*	0.0536

*Minimum mortality rate: 0.0005; #Minimum growth rate: 0.0005.

terms, considered to be 0 as we consider interspecies interaction rather than intra species interaction. The species are considered to have logistic dynamics in which the population increases exponentially.

IV. RESULTS AND ANALYSIS

In this section, we analyze the obtained results by using the aforementioned model. First, we discuss the obtained change detection results. Then, we draw conclusions on the growth rate, survival capacity, and competition between mangrove species.

A. Change Detection of Mangrove Species With Time Series Hyperspectral Data

The accuracy assessment of the changes in mangrove species has been conducted by calculating the RMSE values that are displayed in Table III. To reduce computational complexity in the calculations related to the mixed mangroves, we only considered the singular (linear) interaction part, while ignoring higher order interactions. Geographic locations have been mapped with letters as "A," "B," and "C," as demonstrated in Table III. It can be observed from the abundance estimates in location A that the abundance of *E. agallocha* has increased significantly, while that of *Avicennia officinalis* has slightly increased. In turn, the abundance of *Avicennia alba* and *B. cylindrica* have decreased significantly in the considered three years. The abundance of *E. agallocha*, *C. decandra*, and *Phoenix paludusa* has increased significantly in location B, whereas *A. officinalis* has been observed to decrease from 2011 to 2014. The abundance of *E. agallocha* has increased from 0 to 25% in location C. There has been a significant increase in abundance of *A. alba* and decrease in abundance of *A. officinalis* in this coordinate. A pure mangrove patch of *A. marina* in 2011 at location D shows a decrease in abundance in 2014 with inclusions of *Excoecaria* and *Phoenix* within it.

B. Growth Rate of Relevant Mangrove Species

A detailed analysis of mangrove species dominance has been conducted by exploiting the results provided by spectral unmixing. Specifically, reproduction rate and survival capacities of individual mangrove species have been derived from the abundance estimates of endmembers. In addition, the growth rate has been calculated from the changes derived from the hyperspectral data of 2011 and 2014, respectively. It should be noted that we assume that the mortality rate of mangrove species does not change with time. That is, the mortality rate is the same in 2011 and in 2014. Finally, the growth rate, mortality rate, and reproduction rate of certain locations are reported on Table IV, showing the survival capacity of mangrove species (in certain locations of the study area) and the Importance Value, under an analysis of the equilibrium of the mangrove ecosystem has been expressed by varying survival capacities (K_i and K_j) and interaction coefficients (a_{ij} and a_{ji}), respectively. Notice that the IV is a parameter that indicates the dominance of a particular species over another. The higher the IV of a species, the more it dominates in the area.

TABLE IV
SURVIVAL CAPACITY AND IMPORTANCE VALUES OF MIXED MANGROVE SPECIES

Geographic Location	Name of Species	Survival Capacity (k)	IV
A	*E.agallocha*	0.3945	74.7413
	A. officinalis	0.0028	9.7746
	A. alba	0.0424	9.1463
	B. cylindrica	0.0037	6.3378
B	*E. agallocha*	0.1350	29.4940
	C. decandra	0.1621	35.5918
	P. paludosa	0.1620	34.9142
C	*E. agallocha*	0.3924	72.5857
	A. alba	0.0020	6.1939
	B. cylindrica	0.0030	4.7645
	A. officinalis	0.0890	16.4559

TABLE V
COMPETITION COEFFICIENTS OF MANGROVE SPECIES AT GEOGRAPHICAL LOCATION A

Name of Species	*E. agallocha*	*A. officinalis*	*B. cylindrica*	*A. alba*
E. agallocha	0	1.0008	1.0297	1.0014
A. officinalis	1.0448	0	1.2269	1.0105
B. cylindrica	2.9812	1.2591	0	1.0112
A. alba	1.1912	1.0250	1.0234	0

A detailed analysis of Table IV indicates that *E. agallocha* is the most dominant and important species on the 900 square meter area at geographic Location A. *A. officinalis* is the next dominant species in that region, followed by *A. alba*.

The less important species is *B. cylindrica*. The situation in coordinate C is similar. In coordinate B, *Ceriops* is the dominant species followed by *Excoecaria* and *Phoenix*.

The competition coefficients between different species in Locations A, B, and C are displayed in Tables V–VII. After further analysis of the survival capacity values and an evaluation of the coexistence inequalities, it is apparent that certain degrees of disturbances produce changes in equilibrium status.

C. Pair-Wise Competition of Mangrove Species

For further analysis, Table VIII illustrates the pair-wise competition of mangrove species in the three considered locations. As shown in Table VIII, at geographic Location A, it can be ob-

TABLE VI
COMPETITION COEFFICIENTS OF MANGROVE SPECIES AT GEOGRAPHICAL LOCATION B

Name of Species	*E. agallocha*	*C. decandra*	*P. paludosa*
E. agallocha	0	1.2814	1.1369
C. decandra	1.1932	0	1.1135
P. paludosa	1.0977	1.1179	0

TABLE VII
COMPETITION COEFFICIENTS OF MANGROVE SPECIES AT GEOGRAPHICAL LOCATION C

Name of Species	*E. agallocha*	*A. alba*	*B. cylindrica*
E. agallocha	0	1.0004	1.0009
A. alba	1.0536	0	1.0103
B. cylindrica	1.2046	1.0175	0

TABLE VIII
PAIR-WISE COMPETITION AMONG SPECIES

	Competing Species	Species 1 Wins	Species 2 Wins	Unstable	Stable
A	*E. agallocha* versus *A. officinalis*	Yes			
	E. agallocha versus *A. alba*	Yes			
	E. agallocha versus *B. cylindrica*	Yes			
	A. officinalis versus *A. alba*		Yes		
	A. officinalis versus *B. cylindrica*		Yes		
	A. alba versus *B. cylindrica*	Yes			
B	*E. agallocha* versus *C. decandra*			Yes	
	E. agallocha versus *P. paludosa*		Yes		
	C. decandra versus *P. paludosa*			Yes	
C	*E. agallocha* versus *A. alba*	Yes			
	E. agallocha versus *B. cylindrica*	Yes			
	E. agallocha versus *A. officinalis*	Yes			
	A. alba versus *B. cylindrica*	Yes			
	A. alba versus *A. officinalis*		Yes		
	B. cylindrica versus *A. officinalis*		Yes		

served that *E. agallocha* exhibits the most stable state behavior when in competition with *A. officinalis*, *A. alba,* and *B. cylindrica*. *A. officinalis* is the next dominant species in that pixel coordinates, followed by *A. alba*. At Location B, *Excoecaria* and *Ceriops* exhibit the same strength to compete with each other. An unstable state at this location indicates that there is a possibility of dominance of either species in this region. However, competition between *E. agallocha* and *Phoenix* indicates that Phoenix is the stronger species among them. At location C, the area is dominated by *E. agallocha* and the second most dominant species is *A. officinalis* followed by *A. alba* and *B. cylindrica*. It is thus observed that on analysis of competition between mangrove species over the study area using time series data of 2011 and 2014, *E. agallocha*, *A. officinalis,* and *A. alba* have a better success rate of survival over other mangrove species in the study area.

TABLE IX
GROWTH RATE OF SPECIES IN COMPETITION, CALCULATED USING THE LOTKA–VOLTERRA MODEL

Geographic Location	Name of Species	Growth Rate
A	*E. agallocha*	0.0102
	A. officinalis	0.0010
	A. alba	0
	B.cylindrica	0
B	*E. agallocha*	0.0004
	C. decandra	0.0042
	P. paludosa	0.0029
C	*E. agallocha*	0.0500
	A. alba	0
	B. cylindrica	0
	A. officinalis	0.0103

D. Growth Rate of Species in Competition using the Lotka–Volterra Model

Finally, Table IX presents the growth rate of mangrove species in competition based on the Lotka–Volterra model. It can be observed that the application of Lotka–Volterra model at geographic Location A registers *E. agallocha* to have the fastest species growth rate when paired with *A. alba*, *A. officinalis,* and *B. cylindrica*. It shows a slower growth rate in terms of competition, when paired with *A. officinalis*. The growth rate of *E. agallocha* at this location also emphasizes its dominance over other species within a 3-year time frame, followed by *A. officinalis*. Location B indicates a maximum growth rate of *C. decandra* when in competition with *E. agallocha* and *P. paludosa*. *Phoenix*, when paired with *Excoecaria*, shows a higher growth rate at the same location. At Location C, *E. agallocha* is also the dominant species when compared with *A. alba*, *B. cylindrica,* and *A. officinalis*. However, *A. alba* and *B. cylindrica* do not show any increase in growth over the considered period of time. *A. alba* and *B. cylindrica* have emerged as inferior competitors. *E. agallocha* emerges as a superior competitor among all other mangrove species within the area.

V. CONCLUSION AND FUTURE RESEARCH

We have developed a technique based on the analysis of hyperspectral data to obtain the fractional abundance of pure and mixed mangrove species at subpixel levels. Using this technique, we analyzed the interspecies competition in a selected study area over a period of time. The adopted competition model has been uniquely implemented by exploiting hyperspectral data, and provides insightful information about the behavior of competing mangrove species. The model has helped to predict mangrove species that dominate over others and will survive with time. This study has also exploited a simple linear spectral unmixing model to estimate fractional abundances of mangrove species and used the resulting values as input to derive impor-

tant parameters such as relative dominance, IV of individual mangrove species, and their survival capacity in the study area. The considered model has successfully identified the dominant and dominated species of the pixel areas. The Lotka–Volterra competition model has also helped to provide insightful comparisons between competing mangrove species and to predict the spatio–temporal variations over a period of a few years. Based on the exhaustive analysis of results reported in this paper, it has been observed that *E. agallocha, A. officinalis,* and *C. decandra* are the most dominant species, followed by *Phoenix* and *B. cylindrica*. It is also noted that the existence of dominant mangrove species in the same area, such as *E. agallocha* and *C. decandra*, leads to an unstable condition, as they have the same strength to compete with each other.

In summary, the main novelty of our study is the application of image-derived fractional abundance values obtained from spectral unmixing of hyperspectral data to analyze dynamic mangrove ecosystems using well-founded competition models. In this regard, the use of hyperspectral imagery to predict the equilibrium state of mangrove species represents an original contribution that has not been explored in the literature thus far.

The obtained results are expected to help in the formulation of a plan for conservation and management of mangroves and preparing a framework for their regeneration and restoration in the study area. The uniqueness of this model resides in the application of fractional abundance estimates obtained from spectral unmixing of hyperspectral data for prediction of the ecological dynamics of the mangrove species. This framework is expected to offer a scientific insight for further modeling of ecodynamics in other forest areas.

REFERENCES

[1] M. Demuro and L. Chisholm, "Assessment of hyperion for characterizing mangrove communities," in *Proc. 12th JPL AVIRIS Airborne Earth Sci. Workshop*, Pasadena, CA, USA, 2003, pp.18–23.

[2] C. Vaiphasa, S. Ongsomwang, T. Vaiphasa, and A. K. Skidmore, "Tropical mangrove species discrimination using hyperspectral data: A laboratory study," *Estuarine Coastal Shelf Sci*., vol. 65, no. 1, pp. 371–379, 2004.

[3] C. Vaiphasa, "Remote sensing techniques for mangrove mapping (thesis)," M.S. thesis, Wageningen Univ., Wageningen, The Netherlands, 2005.

[4] W. Koedsin and C. Vaiphasa, "Discrimination of tropical mangroves at the species level with EO-1 Hyperion data," *Remote Sens*., vol. 5, no. 7, pp. 3562–3582, 2013.

[5] T. Wang, H. Zhang, H. Lin, and C. Fang, "Textural–spectral feature based species classification of mangroves in Mai Po Nature reserve fromworldview-3 imagery," *Remote Sens*., vol. 8, no. 24, pp. 1–15, 2016.

[6] G. Viennois *et al.*, "Multi-temporal analysis of high-spatial-resolutionoptical satellite imagery for mangrove species mapping in Bali, Indonesia," *IEEE J. Sel. Topics Appl. Earth Observ. Remote Sens.*, vol. 9, no. 8, pp. 3680–3686, Aug. 2016.

[7] A. R. Frederick and J. Mosquera, "Is space necessary? Interference competition and limits to biodiversity," *Ecology*, vol. 81, no. 11, pp. 3226–3232, 2000.

[8] C. Dislich, K. Johst, and A. Huth, "What enables coexistence in plant communities? Weak versus strong species traits and the role of local processes," *Ecol. Model*., vol. 221, no. 19, pp. 2227–2236, 2010.

[9] R. John, H. S. Dattaraja, H. S. Suresh, and R. Sukumar, "Density-dependence in common tree species in a tropical dry forest in mudumalai, southern India," *J. Vegetation Sci.*, vol. 13, no. 1, pp. 45–56, 2010.

[10] D. Tilman, "Competition and biodiversity in spatially structured habitats," *Ecology*, vol. 75, no. 1, pp. 2–16, 1994.

[11] M. Hussain, D. Chen, A. Cheng, H. Wei, and D. Stanley, "Change detection from remotely sensed images: From pixel-based to object-based approaches," *ISPRS J. Photogramm. Remote Sens.*, vol. 80, pp. 91–106, 2013.

[12] Z. Shaoqing and X. Lu, "The comparative study of three methods of remote sensing image change detection," *Int. Archives Photogramm., Remote Sens. Spatial Inf. Sci.*, vol. 37, no. B7, pp. 1–4, 2008.

[13] S. Singh and R. A. Talwar, "Comparative study on change vector analysis based change detection techniques," *Sadhan*, vol. 39, no. 6, pp. 1311–1331, 2014.

[14] V. Kumar and K. D. Garg, "Valuable approach for image processing and change detection on synthetic aperture radar data," *Int. J. Current Eng. Technol.*, vol. 3, no. 2, pp. 512–516, 2013.

[15] T. Celik, "Unsupervised change detection in satellite images using principal component analysis and means clustering," *IEEE Geosci. Remote Sens. Lett.*, vol. 6, no. 4, pp. 772–776, Apr. 2009.

[16] V. Gulati and P. A. Pal, "Survey on various change detection techniques for hyperspectral images," *Int. J. Adv. Res. Comput. Sci. Softw. Eng.*, vol. 4, no. 8, pp. 852–855, 2014.

[17] X. Benlin, L. Fangfang, M. Xingliang, and J. Huazhong, "Study on independent component analysis application in classification and change detection of multispectral images," *Int. Archives Photogramm., Remote Sens. Spatial Inf. Sci.*, vol. XXXVII, no. Part B7, pp. 871–875, 2008.

[18] M. T. Eismann, M. Joseph, and R. C. Hardie, "Hyperspectral change detection in the presence of diurnal and seasonal variations," *IEEE Trans. Geosci. Remote Sens.*, vol. 46, no. 1, pp. 237–249, Jan. 2008.

[19] C. Wu, B. Du, and L. Zhang, "A subspace-based change detection method for hyperspectral images," *IEEE J. Sel. Topics Appl. Earth Observ. Remote Sens.*, vol. 6, no. 2, pp. 815–830, Feb. 2013.

[20] K. Tan, X. Jin, A. Plaza, X. Wang, L. Xiao, and P. Du, "Automatic change detection in high-resolution remote sensing images by using a multiple classifier system and spectral-spatial features," *IEEE J. Sel. Topics Appl. Earth Observ. Remote Sens.*, vol. 9, no. 8, pp. 3439–3451, Aug. 2016.

[21] A. Erturk, M. D. Iordache, and A. Plaza, "Sparse unmixing based change detection for multi-temporal hyperspectral images," *IEEE J. Sel. Topics Appl. Earth Observ. Remote Sens.*, vol. 9, no. 2, pp. 708–719, Feb. 2016.

[22] I. M. Bomze, "Lotka–Volterra equation and replicator dynamics: A two-dimensional classification," *Biol. Cybern*., vol. 48, pp. 201–211, 1983.

[23] I. M. Bomze, "Lotka–Volterra equation and replicator dynamics: New issues in classification," *Biol. Cybern*., vol. 72, pp. 447–453, 1995.

[24] J. C. Sprott, J. C. Wildenberg, and Y. Azizi, "A simple spatiotemporal chaotic lotka–volterra model. Chaos," *Solitons & Fractals*, vol. 26, p. 1035, 2005.

[25] J. R. Jensen, *Introductory Digital Image Processing: A Remote Sensing Perspective*. Pearson, Englewood Cliffs, NJ, USA: Prentice Hall, 1996.

[26] A. Plaza, P. Martínez, R. Pérez, and J. A. Plaza, "Quantitative and comparative analysis of endmember extraction algorithms from hyperspectral data," *IEEE Trans. Geosci. Remote Sens.*, vol. 42, no. 3, pp. 650–663, Mar. 2004.

[27] N. Keshava and J. F. Mustard, "Spectral unmixing," *IEEE Signal Process. Mag.*, vol. 19, no. 1, pp. 44–57, Jan. 2002.

[28] S. Chakravortty, "Analysis of endmember detection and subpixel classification algorithms onhyperspectral imagery for tropical mangrove species discrimination in the Sunderbans Delta, India," *J. Appl. Remote Sens.*, vol. 7, no. 1, 2013, Art no. 073523.

[29] X. Xu, X. Tong, A. Plaza, Y. Zhong, H. Xie, and L. Zhang, "Using linear spectral unmixing for sub-pixel mapping of hyperspectral imagery: A quantitative assessment," *IEEE J. Sel. Topics Appl. Earth Observ. Remote Sens.*, vol. 10, no. 4, pp. 1589–1600, Apr. 2017.

[30] A. Erturk, M. D. Iordache, and A. Plaza, "Sparse unmixing with dictionary pruning for hyperspectral change detection," *IEEE J. Sel. Topics Appl. Earth Observ. Remote Sens.*, vol. 10, no. 1, pp. 321–330, Jan. 2017.

[31] W. Luo *et al.*, "A new algorithm for bilinear spectral unmixing of hyperspectral images using particle swarm optimization," *IEEE J. Sel. Topics Appl. Earth Observ. Remote Sens.*, vol. 9, no. 12, pp. 5776–5790, Dec. 2016.

[32] L. Zhuang, B. Zhang, L. Gao, J. Li, and A. Plaza, "Normal endmember spectral unmixing method for hyperspectral imagery," *IEEE J. Sel. Topics Appl. Earth Observ. Remote Sens.*, vol. 8, no. 6, pp. 2598–2606, Jun. 2015.

[33] P. T. Obade *et al.*, "Impact of anthropogenic disturbance on a mangrove forest assessed by a 1d cellular automaton model using Lotka–Volterra-type competition," *Int. J. Des. Nature Ecodyn.*, vol. 3, no. 4, pp. 296–320, 2009.

[34] J. T. Curtis (ed.), *The Vegetation of Winsconsin. An Ordination of Plant Communities*. Madison, WI, USA: Univ. of Wisconsin Press, 1959.

Somdatta Chakravortty received the B.Tech. degree in civil engineering from Kanpur University, Kanpur, India, in 1997, the M.Tech. degree in information technology from Bengal Engineering and Science University, Sibpur, India, in 2002, and the Ph.D. degree in computer science and engineering from Calcutta University, Kolkata, India, in 2017.

She is currently an Assistant Professor in Information Technology and is with the Government College of Engineering and Ceramic Technology, Kolkata. She has worked in the industry for four years and has been teaching in engineering colleges since 2003 till date. She has authored several research papers in international and national journals, book chapters, international and national level conferences. She has several research projects funded by the Department of Science and Technology, University Grants Commission, and All India Council of Technical Education, Govt. of India, which focuses on research related to hyperspectral image analysis. Her current research interests include hyperspectral image analysis, algorithm development and image fusion.

Dr. Chakravortty is a member of professional societies such as the Indian Society of Remote Sensing, the Computer Society of India, and the Institute of Engineers and is actively involved in organising chapter-related activities of the society.

Jun Li (SM'16) received the B.S. degree in geographic information systems from Hunan Normal University, Changsha, China, in 2004, the M.E. degree in remote sensing from Peking University, Beijing, China, in 2007, and the Ph.D. degree in electrical engineering from the Instituto de Telecomunicações, Instituto Superior Técnico (IST), Universidade Técnica de Lisboa, Lisbon, Portugal, in 2011.

She is currently a Professor with Sun Yat-sen University, Guangzhou, China, where she founded her own research group on hyperspectral image analysis and calibration in 2013. Since then, she has obtained several prestigious funding grants at the national and international level. She has authored or coauthored a total of 68 journal citation report (JCR) papers, 48 conference international conference papers, and 1 book chapter. She has received a significant number of citations to her published works, with several papers distinguished as "Highly Cited Papers" in Thomson Reuters' Web of Science Essential Science Indicators (WoS-ESI). Her students have also obtained important distinctions and awards at international conferences and symposia. She has been a Guest Editor for several journals, including the *ISPRS Journal of Photogrammetry and Remote Sensing*. She has also been an active reviewer for several journals, including *Pattern Recognition*, *Optical Engineering*, *Journal of Applied Remote Sensing,* and *Inverse Problems and Imaging.* Her current research interests include remotely sensed hyperspectral image analysis, signal processing, supervised/semisupervised learning, and active learning.

Prof. Li is an Associate Editor for the IEEE JOURNAL OF SELECTED TOPICS IN APPLIED EARTH OBSERVATIONS AND REMOTE SENSING (since 2014). She has been a Guest Editor for several journals, including the PROCEEDINGS OF THE IEEE. She has also been an active reviewer for several journals, including the IEEE TRANSACTIONS ON GEOSCIENCE AND REMOTE SENSING, the IEEE GEOSCIENCE AND REMOTE SENSING LETTERS, and the IEEE TRANSACTIONS ON IMAGE PROCESSING. She has received several important awards and distinctions, including the IEEE Geoscience and Remote Sensing Society (GRSS) Early Career Award in 2017, due to her outstanding contributions to remotely sensed hyperspectral and synthetic aperture radar data processing. She was also distinguished as one of the best self-funded Chinese students abroad by the Chinese Scholar Council (in 2010). She was distinguished as a Best Reviewer of the IEEE JOURNAL OF SELECTED TOPICS IN APPLIED EARTH OBSERVATIONS AND REMOTE SENSING (in 2013). One of her students received the Best Student Paper at the 2016 *SPIE Remote Sensing Europe Symposium* held in Edinburgh, UK for the contribution "A New Tool for Unsupervised Classification of Satellite Images Available on Web Servers: Google Maps as a Case Study" (in September 2016). One of her students received the second prize in the Student Paper competition held at the 2017 *IEEE International Geoscience and Remote Sensing Symposium* (IGARSS) held in Fort Worth, TX, USA, for the contribution "Hyperspectral Cloud Shadow Removal Based on Linear Unmixing"(in July 2017).

Antonio Plaza (M'05–SM'07–F'15) received the M.Sc. and the Ph.D. degrees both in computer engineering from the Hyperspectral Computing Laboratory, Department of Technology of Computers and Communications, University of Extremadura, Badajoz, Spain, in 1999 and 2002, respectively.

He is currently the Head of the Hyperspectral Computing Laboratory, Department of Technology of Computers and Communications, University of Extremadura. He has authored or coauthored more than 600 publications, including more than 200 JCR journal papers (over 150 in IEEE journals), 24 book chapters, and over 300 peer-reviewed conference proceeding papers. He has guest edited 10 special issues on hyperspectral remote sensing for different journals. He has reviewed more than 500 papers for over 50 different journals. His current research interests include hyperspectral data processing and parallel computing of remote sensing data.

Prof. Plaza is a Fellow of IEEE "for contributions to hyperspectral data processing and parallel computing of Earth observation data." He is a recipient of the recognition of Best Reviewers of the IEEE GEOSCIENCE AND REMOTE SENSING LETTERS (in 2009) and a recipient of the recognition of Best Reviewers of the IEEE TRANSACTIONS ON GEOSCIENCE AND REMOTE SENSING (in 2010), for which he served as Associate Editor in 2007–2012. He is also an Associate Editor for the IEEE Access and was a member of the Editorial Board of the IEEE GEOSCIENCE AND REMOTE SENSING NEWSLETTER (2011–2012) and the IEEE GEOSCIENCE AND REMOTE SENSING MAGAZINE (2013). He was also a member of the Steering Committee of the IEEE JOURNAL OF SELECTED TOPICS IN APPLIED EARTH OBSERVATIONS AND REMOTE SENSING (JSTARS). He is a recipient of the Best Column Award of the IEEE SIGNAL PROCESSING MAGAZINE in 2015, the 2013 Best Paper Award of the JSTARS journal, and the most highly cited paper (2005–2010) in the *Journal of Parallel and Distributed Computing*. He received the Best Paper Awards at the IEEE International Conference on Space Technology and the IEEE Symposium on Signal Processing and Information Technology. He served as the Director of Education Activities for the IEEE Geoscience and Remote Sensing Society (GRSS) in 2011–2012 and as President of the Spanish Chapter of IEEE GRSS in 2012–2016. He has served as the Editor-in-Chief of the IEEE TRANSACTIONS ON GEOSCIENCE AND REMOTE SENSING journal from 2013 to 2017. (Additional information: http://www.umbc.edu/rssipl/people/aplaza)